



Cite this: *Biomater. Sci.*, 2020, **8**, 6301

Peptide modified polycations with pH triggered lytic activity for efficient gene delivery†

Xiaojing Chen,^a Kai Xu,^a Jing Yu,^a Xiaodan Zhao,^b Qiang Zhang,^a Yanfeng Zhang ^a and Yilong Cheng *^a

Endo/lysosome entrapment is the key barrier for gene delivery using synthetic polycations. Although the introduction of a membrane-lytic peptide into polycations could facilitate efficient endo/lysosome release and improve gene delivery efficiency, it is always accompanied by serious safety concerns. In this work, the widely used polycations, poly(2-dimethylaminoethyl methacrylate) (PDMAEMA), poly(L-lysine) (PLL) and polyethylenimine (PEI), are modified with a pH-sensitive peptide (C6M3) with selective lytic activity to produce three functional polycations to address the issue of endo/lysosome entrapment and facilitate efficient gene transfer. Hemolysis study shows that the functionalized polycations show good biocompatibility toward red blood cells at neutral pH, and exhibit potent membrane lysis activity under acidic conditions, which are both on-demand for the ideal gene carriers. *In vitro* transfection studies demonstrate that the peptide modified polycations mediate promising gene delivery efficiency with the luciferase plasmid and the green fluorescence protein plasmid in HeLa cells compared to the parent polycations. Owing to the facile preparation and selective lysis activity of the C6M3 modified polycations, these smart gene vectors may be good candidates for the transfer of various nucleic acids and further clinical gene therapy.

Received 24th July 2020,
Accepted 13th September 2020
DOI: 10.1039/d0bm01231a
rsc.li/biomaterials-science

1. Introduction

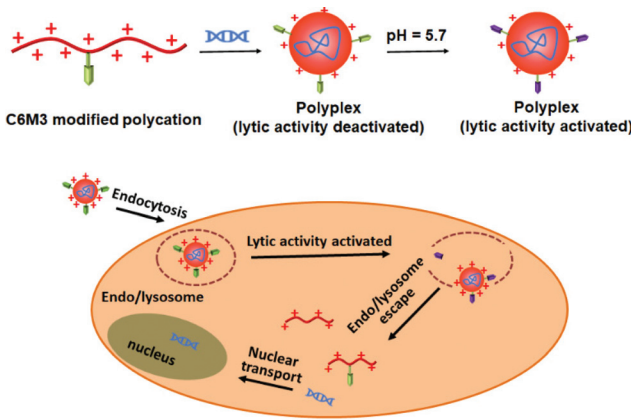
Delivery of therapeutic nucleic acids into target cells is regarded as an efficient way to tackle a myriad of acquired or congenital diseases.^{1–6} However, the poor stability under physiological conditions and the impermeability of cell membranes to nucleic acids significantly compromise the gene therapy efficiency. Hence, the assistance of a carrier to successfully transfer nucleic acids into the intracellular parts is of importance for gene delivery.^{7–12} Compared to viral carriers, non-viral carriers, especially polycations, feature various advantages, such as affordable facile preparation and functionalization, low immunogenicity and inflammation, which have been widely employed for the delivery of plasmid DNA (pDNA),^{13–17} small interfering RNA (siRNA),^{18–24} messenger RNA (mRNA) and micro RNA (miRNA).^{25–31} However, due to the limited capability to overcome various physiological barriers, the gene delivery efficiency is usually orders of magnitude lower than those of their viral counterparts.^{32–35}

Endo/lysosome entrapment is the key obstacle for polycation-based intracellular gene delivery.³⁶ If the formed complexes of nucleic acids and polycations are trapped in the endosome and cannot escape in time, it will be automatically routed into lysosome degradation, leading to failed gene transfer.^{37–39} Tremendous efforts have been made to address this issue.^{40–45} The proton sponge effect is the widely used method for polycation mediated endosomal release.^{46,47} However, it cannot be translated into *in vivo* applications due to the requirement of a large amount of polymer accumulation in the endo/lysosome, which may raise safety concerns. As an alternative way, peptides with membrane-lytic activity, such as melittin and sHGP, have been introduced into polycations to facilitate endo/lysosomal escape.^{48–50} The peptide-conjugated polymers can significantly improve the gene delivery efficiency compared to the parent polymers. But due to off-site lysis, serious cytotoxicity was also detected. We recently designed a pH-sensitive block copolymer, called VIPER (virus-inspired polymer for endosomal release), aiming to minimize the side effect.^{28,42} VIPER can assemble into nanoparticles with a lytic peptide shielded in the core; that responds to endosomal acidification by revealing a membrane-lytic peptide that is conjugated to a reversibly hydrophobic polymer block, followed by promising gene transfer efficiency in various cell lines *in vitro* and different tissues *in vivo*. However, the cleavage of the disulfide linkage between melittin and the polymer may raise

^aSchool of Chemistry, Xi'an Jiaotong University, Xi'an 710049, China.
E-mail: yilongcheng@mail.xjtu.edu.cn

^bKey Laboratory of Shaanxi Province for Craniofacial Precision Medicine Research, College of Stomatology, Xi'an Jiaotong University, Xi'an 710049, China

† Electronic supplementary information (ESI) available. See DOI: [10.1039/d0bm01231a](https://doi.org/10.1039/d0bm01231a)



Scheme 1 Illustration of C6M3 modified polycations for successful gene delivery.

undesired safety concerns because of the native lytic activity of melittin under physiological conditions.⁵¹

Previous studies showed that the C6M3 peptide (a peptide derived from C6) features pH-triggered lytic activity, and promising membrane lysis was observed under endo/lysosomal acidic conditions rather than at a normal pH value.^{51,52} We hypothesize that the incorporation of polycations with C6M3 could not only enhance the gene delivery efficiency through the promotion of endo/lysosomal escape but also avoid off-site toxicity. As shown in Scheme 1, the C6M3 modified polycations condense DNA into nanoparticles, which can be endocytosed by cells through the endosome pathway. Afterward, C6M3 can be activated to mediate endo/lysosomal escape of the polyplexes. In this work, three widely used polycations, poly(2-dimethylaminoethyl methacrylate) (PDMAEMA), poly(L-lysine) (PLL) and branched polyethylenimine (PEI), are modified with the C6M3 peptide (Fig. 1), and the pH selective hemolysis was evaluated with mouse red blood cells to verify the desired membrane-lytic activity. The functionalized polycations are also well assessed. To explore the potential for gene therapy, the luciferase plasmid and the green fluorescence protein (GFP) plasmid as reporter genes are employed to evaluate the gene delivery efficiency of the polycations *in vitro*.

The chemical and biological reagents used in this work are listed in the ESI.†

2. Experimental section

2.1. Materials

The chemical and biological reagents used in this work are listed in the ESI.†

2.2. Characterization

The ¹H nuclear magnetic resonance (¹H NMR) spectra were recorded on a Bruker Avance 400 spectrometer (400 MHz). The size and surface charge of the polyplexes were tested on a Malvern ZEN 3690 system. The morphology of all the polyplexes in the dried state was imaged with a JEOL JEM-2100 electron microscope using an acceleration voltage of 120 kV. UV-vis absorption spectra were measured with a Shimadzu UV-2550 spectrometer.

2.3. Polymer synthesis

2.3.1. Synthesis of PDMAEMA-*co*-PDSEMA. Pyridyl disulfide ethyl methacrylate (PDSEMA) (9.14 mg, 7.2 mmol), 2-(dimethylamino)ethyl methacrylate (DMAEMA) (557 mg, 64.5 mmol), *N,N*-azobisisobutyronitrile (AIBN) (3.92 mg, 0.072 mmol) and 4-cyanopentanoic acid dithiobenzoate (CPADB) (10 mg, 0.072 mmol) were dissolved in dioxane (896 μL). After purging with nitrogen for 30 min, the polymerization was initiated in an oil bath at 70 °C and the mixture was stirred for 24 h. The monomer conversion was monitored by ¹H NMR spectroscopy. The polymerization was quenched by immersing the reaction flask in liquid nitrogen. The polymer, PDMAEMA-*co*-PDSEMA, was collected by three cycles of dissolving/precipitating with dichloromethane/hexane.

2.3.2. Synthesis of PLL-SPDP. PLL was synthesized according to the previous work.⁵³ The degree of polymerization was 44 determined by ¹H NMR spectroscopy. 3-(Pyridin-2-ylsulfonyl)propanoic acid (PDSPA) was synthesized as shown in Scheme S1 in the ESI.† PDSPA (0.039 g, 0.18 mmol) was first dissolved in a mixture of DMSO and water (1 mL) followed by the addition of EDC (0.036 g, 0.19 mmol) and NHS (0.022 g, 0.19 mmol). The reaction mixture was stirred at room temperature for 0.5 h to obtain 3-(2-pyridylthio)propionic acid *N*-hydroxysuccinimide ester (SPDP). Afterward, the solution of SPDP was slowly added to PLL (500 mg, 0.09 mmol) dissolved in a mixture of DMSO and water (2 mL), and the reaction mixture was stirred at room temperature for an additional 72 h. PLL-SPDP was obtained by dialysis and lyophilization.

2.3.3. Synthesis of PEI-SPDP. The conjugation of PDSPA to PEI was similar to that for PLL as shown above, and PEI-SPDP was obtained by dialysis and lyophilization.

2.3.4. Synthesis of C6M3 modified polycations. Cys-C6M3 was conjugated to the polycations through a disulfide exchange reaction. For example, PDMAEMA-*co*-PDSEMA

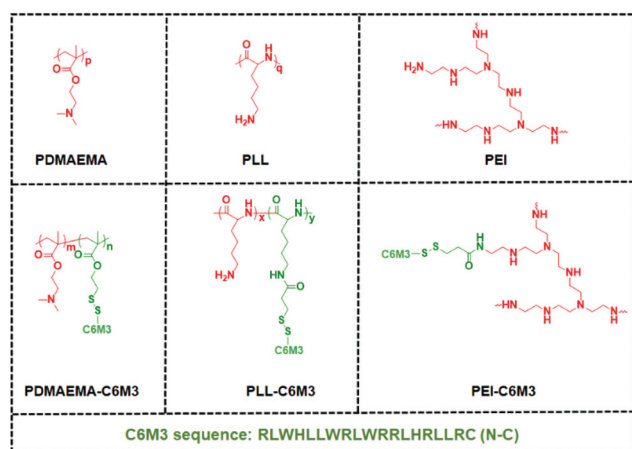


Fig. 1 Chemical structures of the polycations and the sequence of C6M3.

(7.5 mg, 0.001 mmol PDS groups) was dissolved in 2 mL PB (0.2 M, pH 5.7) in a 10 mL flask. Then, 6.1 mg (0.002 mmol, 2 equiv. relative to PDS groups) of cys-C6M3 was added into the flask and allowed to stir under nitrogen at room temperature. The reaction was monitored by UV spectroscopy at 340 nm for the release of 2-thiopyridine. After 24 h, the absorption was saturated and the reaction mixture was passed through a PD-10 column to remove the side product and unreacted peptide followed by lyophilization. The conjugations of C6M3 to PLL-SPDP and PEI-SPDP were performed with the same procedure. The peptide modified polycations were denoted as PDMAEMA-C6M3, PLL-C6M3 and PEI-C6M3.

2.4. Gel retardation

For polyplex preparation, the parent and peptide modified polymer solutions with different concentrations were added to the luciferase plasmid solution (v/v = 1 : 1), and the formed polyplex solutions were vortexed for 15 seconds and incubated at room temperature for 10 min. The polyplex solution (12 μ L) with different N/P ratios was subjected to electrophoresis on agarose gel (1%) at 100 V for 45 min to test the DNA condensing ability.

2.5. Hemolysis of polycations

Hemolysis assay was used to evaluate the acid-triggered membrane-lytic activity of the synthetic materials at pH 7.4 and 5.7. The details are presented in the ESI.[†]

2.6. *In vitro* transfection

Luciferase and GFP plasmids were used to evaluate the gene delivery efficiency of the polycations. HeLa cells were seeded with a density of 20 000 cells per well (24 well plate) in MEM medium supplemented with 10% FBS and 1% antibiotic/antimicrobial. Cells were firstly incubated at 37 °C under 5% CO₂ for 24 h. Polyplexes were prepared at different N/P ratios using 1 μ g of pGL3 in 20 μ L total volume. Each sample was diluted with 180 μ L OptiMEM medium. For transfection study, the cells were washed with PBS, followed by the addition of the polyplex solution. After incubation for 4 h, the cells were rinsed with PBS twice and complete cell culture medium (500 μ L) was added. After an additional 44 h of incubation, luciferase activity was quantified with a luciferase assay kit (Promega Corp, Fitchburg, WI). The total protein content in each well was measured using a BCA Protein Assay Kit. The GFP plasmid delivery study was the same as that with the luciferase plasmid. Flow cytometry was used to analyze the percentage of the transfected cells.⁴² All experiments were conducted in triplicate.

2.7. Statistical analysis

All statistical analyses were performed using a two-tailed Student's *t*-test with unequal variance.

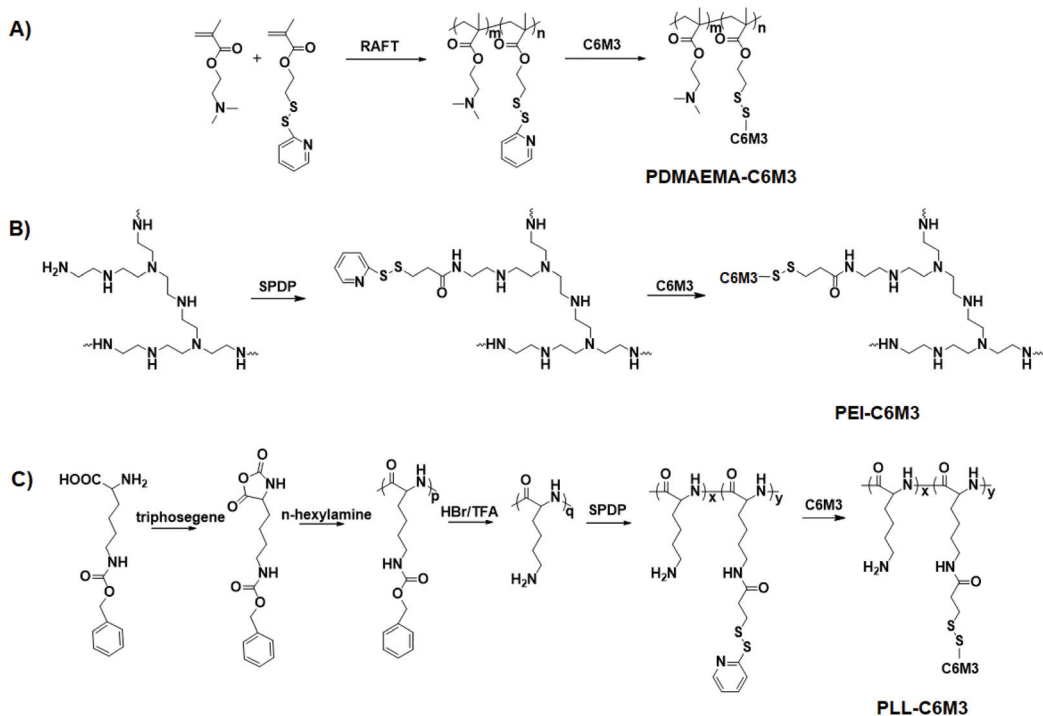
3. Results and discussion

3.1. Polymer synthesis and characterization

The synthetic routes of the polycations are shown in Scheme 2A–C. To synthesize C6M3 modified PDMAEMA, a functional monomer, PDSEMA, was first copolymerized with DMAEMA to afford P(DMAEMA-*co*-PDSEMA). The ¹H NMR spectra are shown in Fig. S1,[†] and all the signals were assigned. The composition of the polymer was determined to be P(DMAEMA₉₈-*co*-PDSEMA₂) based on the conversion (~100%) of the monomers. The GPC results showed that the molecular weight of the copolymer was 218 000, and the polydispersity index was 1.19. PZLL was synthesized by the ring-opening polymerization of 3-benzyloxycarbonyl-L-lysine *N*-carboxyanhydride (ZLL NCA) in the presence of hexylamine. The degree of polymerization of PZLL was determined to be 44 based on the ¹H NMR spectrum (Fig. S2[†]), and the molecular weight of PZLL was 166 000 with a polydispersity index of 1.24. After deprotection in the presence of trifluoroacetic acid, the obtained PLL was used to react with SPDP by EDC/NHS chemistry. Based on the ¹H NMR spectra shown in Fig. S2,[†] there were 1.2 SPDP linked to the side chain of PLL. The SPDP modified PEI was prepared using the same protocol, and the signals at 8.3, 7.8 and 7.2 ppm demonstrated the successful incorporation of SPDP (Fig. S3[†]). We used the UV spectrum to quantify the amount of the functional group (Fig. S4[†]), and the results showed that there was 0.9 PDSPA per PEI. Next, cysteine-C6M3 was introduced into the polycations through a disulfide exchange reaction, and the reactions were monitored by UV spectroscopy (Fig. S5[†]). After 24 h, the absorption was saturated, indicating the completion of the modification. Based on the above results, three C6M3 modified polycations were successfully obtained, and there were 2, 1.2 and 0.9 C6M3 for PDMAEMA, PLL and PEI, respectively.

3.2. Hemolysis testing of the polycations

It is reported that C6M3 exhibits pH dependence for membrane lysis. To verify the pH selective lytic activity, we incubated the peptide modified polycations (10–100 μ g mL^{−1}) with mouse red blood cells at different pH values for 1 h at 37 °C. The absorption at 541 nm attributed to the characteristic peak of hemoglobin in the UV spectrum was then used to quantify the hemolytic activity. As shown in Fig. 2, negligible hemolysis was detected when the concentration of the polymers was lower than 80 μ g mL^{−1} at pH 7.4. However, obvious hemolysis was detected when the pH of the culture media was 5.7, and the lytic activity showed concentration dependence. Previous work demonstrated that the EC₅₀ (the concentration of free peptide for 50% hemolysis) value of C6M3 was ~16 μ g mL^{−1},⁵² which was much lower than those in our work (29.7, 27.0 and 33.8 μ g mL^{−1} for PDMAEMA-C6M3, PEI-C6M3 and PLL-C6M3, respectively). This may be attributed to the fact that the conjugation of C6M3 to polycations compromises the lytic activity. Meanwhile, no obvious hemolysis was observed for PDMAEMA, PEI and PLL at pH 7.4 and 5.7 in the tested concentration range, indicating that membrane lysis is caused by



Scheme 2 Synthetic routes of the polycations. A: PDMAEMA-C6M3; B: PEI-C6M3; C: PLL-C6M3.

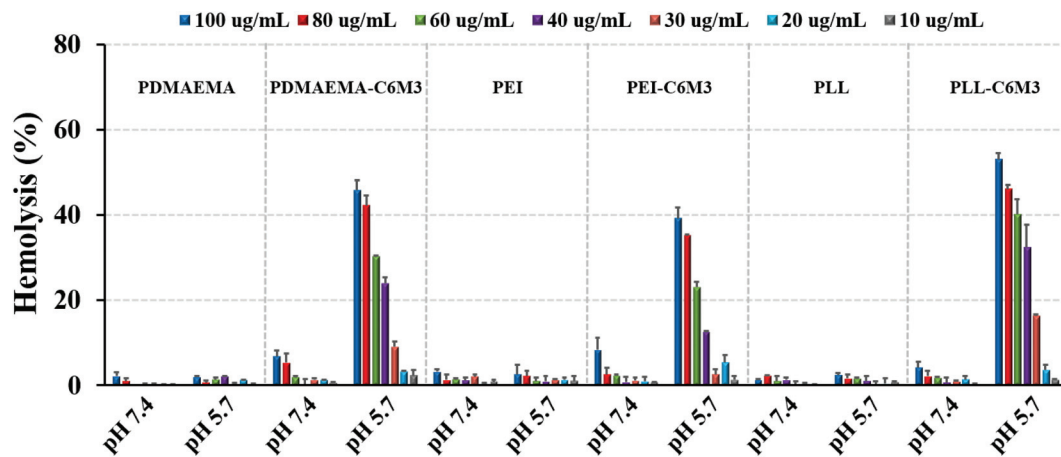


Fig. 2 Hemolysis activity of polycations and C6M3 modified polycations at various concentrations and pH values. Data are shown as mean \pm SD ($n = 3$).

the pH triggered activation of C6M3 rather than the polymer backbone.

3.3. Polyplex characterization

We performed agarose gel electrophoresis assay to evaluate the DNA binding ability of the parent polycations and the C6M3 functionalized polycations. As shown in Fig. S6,† it was observed that all the polymers can completely retard the mobility of DNA when the N/P ratio (amine to phosphate) was higher than 2. Moreover, we found that the introduction of the C6M3 peptide had no obvious effect on the DNA condensing

capability of the polycations. DLS was then employed to test the size of the polyplexes with different N/P ratios. It was found that all the polycations could condense DNA into nanoparticles with the hydrodynamic diameter in the range of 70–200 nm (Fig. 3A), which is beneficial for cellular endocytosis. The increase in the N/P ratio led to a smaller size owing to the enhanced condensing capability. Besides, the incorporation of C6M3 into polycations slightly increased the size of the polyplexes compared to the parent polymers, which may be attributed to the relatively hydrophobic nature of the peptide at neutral pH. Furthermore, the morphology of the

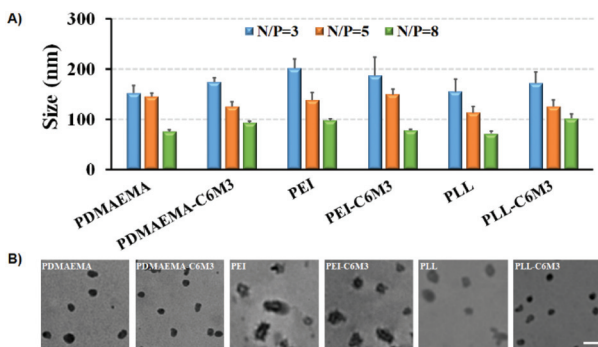


Fig. 3 (A) Average hydrodynamic diameters of different formulations. (B) TEM images of polymer/DNA complexes formed at N/P = 5 (scale bar: 100 nm).

polyplexes was imaged by TEM at an N/P ratio of 5 (Fig. 3B). We can find that all the polyplexes featured compact structures with a relatively uniform spherical shape, and the diameter was around 100 nm. The size based on DLS testing was larger than that obtained by TEM, which may be attributed to the shrinkage of the polyplexes during sample preparation in TEM testing.

The positively charged surface of the nanoparticles is favorable to cellular endocytosis since the cell membrane is negatively charged. The zeta potentials of all the polyplexes were above 20 mV (Fig. 4), which is beneficial for cell membrane binding. And the increase of the N/P ratio resulted in the increase of the zeta potential. Because of the partial shielding of the peptide, the surface charge of the polyplexes by C6M3 modified polyplexes was slightly lower than that by the parent polycations.

3.4. *In vitro* transfection

C6M3 modified polycations not only showed good biocompatibility to cells at neutral pH (negligible hemolysis to red blood cells), but also exhibited promising membrane lysis under acidic conditions, both of which are desirable for an ideal non-viral gene vector. Then we performed the gene transfection study *in vitro* using the luciferase plasmid and the GFP

plasmid as reporter genes in HeLa cells to evaluate the delivery efficiency using the six polycations. As shown in Fig. 5A, for PDMAEMA, the transfection efficiency increased with the N/P ratio from 3 to 8, and the same trend was also observed for PEI. However, the cell viability at the N/P ratio of 8 was lower than 80%, indicating potential cytotoxicity due to the excess polycations. PLL also showed enhanced delivery efficiency when the N/P ratio increased from 3 to 5, but further improvement of the N/P ratio led to compromised luciferase transgene expression, which may be attributed to the hard unpackaging of the payloads in the cytoplasm. When the pH-sensitive peptide was introduced into the polycations, the transfection efficiency was significantly enhanced. The luciferase expression mediated by PDMAEMA-C6M3, PEI-C6M3 and PLL-C6M3 at the N/P ratio of 5 was around 5.7, 3.1 and 7.8 times higher than that by PDMAEMA, PEI and PLL, respectively. The relative cell viability results in Fig. 5B reveal that the polycations showed acceptable cell biocompatibility at N/P ratios of 3 and 5 (>80%).

Furthermore, based on the promising luciferase plasmid delivery efficiency and acceptable cell compatibility mediated by the N/P ratio of 5, we selected the corresponding formulations to deliver the GFP plasmid to quantify the percentage of the transfected cells using a flow cytometer. As shown in Fig. 6, we found that around 22% and 29% cells were transfected by PDMAEMA-C6M3 and PEI-C6M3, which were much higher than those mediated by the parent PDMAEMA and PEI (7.0% and 16.3%). Although the percentage of transfected cells by PLL and PLL-C6M3 was much lower, the obvious improvement also can be observed after the introduction of C6M3 into PLL. Fig. S7† shows the representative results of the flow cytometry analysis. Furthermore, the GFP positive cells in the transfection study were also observed by fluorescence microscopy (Fig. S8†). We can find that cells transfected by the C6M3 modified polycations showed enhanced fluorescence intensity, suggesting that more cells were transfected.

It is reported that melittin modified polycations could improve the gene delivery efficiency owing to the membrane lytic nature, but serious cytotoxicity was observed when the N/P ratio was higher than 3, which was attributed to off-site lysis.⁴⁸ In order to address the off-site toxicity, the Wagner group developed functional polycations with anhydride masked melittin to selectively shield the undesirable lysis for gene delivery. The resulting polycations can deactivate the peptide at neutral pH, and mediated successful endosomal escape of the polyplexes through the acidic pH triggered hydrolysis of the anhydride, further leading to promising siRNA delivery efficiency.⁴³ Although acceptable biocompatibility and excellent delivery efficiency were achieved, the anhydride protecting group is reversible and susceptible to hydrolysis even at neutral pH,⁵⁴ which may raise safety issues during long-term storage. Since C6M3 features pH selective lytic activity, the modified polycations could avoid the toxicity toward cells extracellularly; in the acidic endo/lysosomal environment, the activated lysis capability induces the disruption of the mem-

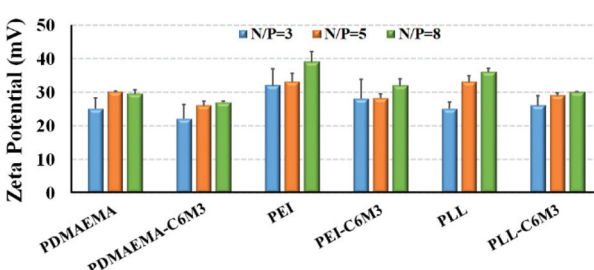


Fig. 4 Zeta potential of different formulations. Data are shown as mean \pm SD ($n = 3$).

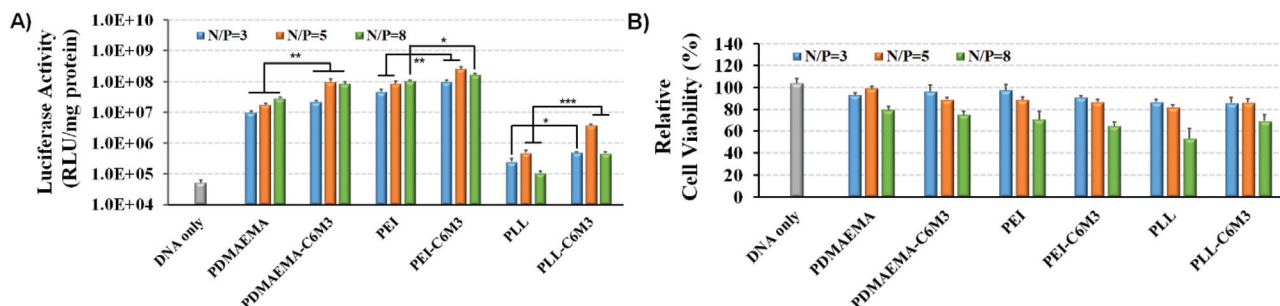


Fig. 5 *In vitro* transfection with HeLa cells with various polyplexes at different N/P ratios. (A) Transfection efficiency. (B) Relative cell viability. Data are shown as mean \pm SD ($n = 3$; Student's *t*-test, * $p < 0.05$, ** $p < 0.01$, *** $p < 0.001$).

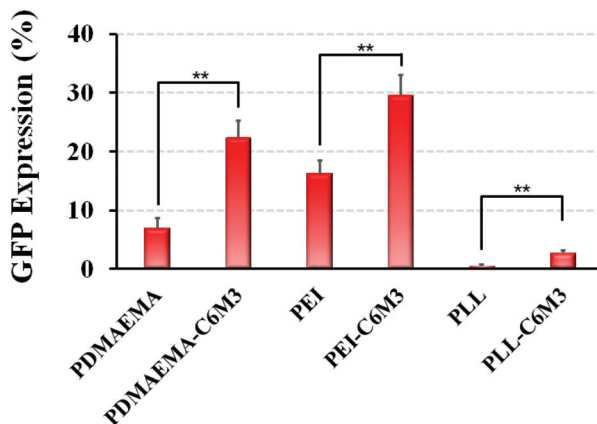


Fig. 6 *In vitro* GFP plasmid delivery efficiency with HeLa cells using different polyplexes (N/P = 5). Data are shown as mean \pm SD ($n = 3$; Student's *t*-test, ** $p < 0.01$).

brane structure and facilitates efficient escape from endo/lysosome entrapment. Furthermore, the peptide can be de-activated again after release, and recover the safe nature. Hence, our C6M3 modified polycations could realize successful nucleic acid delivery while avoiding off-site cytotoxicity, which may endow the polycations with outstanding advantages for clinical applications.

4. Conclusions

In summary, three widely used polycations (PDMAEMA, PLL and PEI) functionalized with a pH-sensitive peptide C6M3 were employed as gene vectors to mediate efficient endo/lysosome release and further successful gene delivery. PDMAEMA-C6M3, PLL-C6M3 and PEI-C6M3 showed selective membrane lysis behavior under endo/lysosomal acidic conditions, and did not cause off-site safety concerns as the parent polycations. Furthermore, *in vitro* transfection results demonstrated that the C6M3 modified polycations exhibited higher gene transfer capability using luciferase and GFP plasmids in HeLa cells than that by the parent polycations with good biocompatibility. Our work provides a facile, safe and

efficient way to address the issue of endo/lysosome entrapment for polycation-based gene therapy, and may promote the translation of non-viral vectors for clinical applications.

Conflicts of interest

There are no conflicts to declare.

Acknowledgements

The authors acknowledge the financial support from the National Natural Science Foundation of China (NSFC 51803165), the Natural Science Basic Research Plan in Shaanxi Province of China (2019JQ-167), the “Young Talent Support Plan” of Xi'an Jiaotong University, and the Fundamental Research Funds for the Central Universities (xjj2018050). We also acknowledge the support of the Opening Project of Key Laboratory of Shaanxi Province for Craniofacial Precision Medicine Research, College of Stomatology, Xi'an Jiaotong University (2019LHM-KFKT007).

Notes and references

- 1 C. E. Dunbar, K. A. High, J. K. Joung, D. B. Kohn, K. Ozawa and M. Sadelain, *Science*, 2018, **359**, eaan4672.
- 2 Y. Liu, C. F. Xu, S. Iqbal, X. Z. Yang and J. Wang, *Adv. Drug Delivery Rev.*, 2017, **115**, 98–114.
- 3 L. J. Chang and A. S. Lewin, *Curr. Gene Ther.*, 2018, **18**, 1–1.
- 4 S. L. Ginn, A. K. Amaya, I. E. Alexander, M. Edelstein and M. R. Abedi, *J. Gene Med.*, 2018, **20**, e3015.
- 5 L. Naldini, *Nature*, 2015, **526**, 351–360.
- 6 Y. Yang, B. Xue, K. Shi, Y. Jia, Y. Hao, Y. Xiao and Z. Qian, *J. Biomed. Nanotechnol.*, 2019, **15**, 431–442.
- 7 M. F. Naso, B. Tomkowicz, W. L. Perry and W. R. Strohl, *BioDrugs*, 2017, **31**, 317–334.
- 8 L. Peng and E. Wagner, *Biomacromolecules*, 2019, **20**, 3613–3626.
- 9 D. Pepin, A. Sosulski, K. Hendren, L. H. Zhang, F. Nicolaou, D. Wang, G. P. Gao and P. K. Donahoe, *Clin.*

Cancer Res., 2015, **21**, DOI: 10.1158/1557-3265.OVCASYMP14-AS25.

10 H. Wei, L. R. Volpatti, D. L. Sellers, D. O. Maris, I. W. Andrews, A. S. Hemphill, L. W. Chan, D. S. H. Chu, P. J. Horner and S. H. Pun, *Angew. Chem., Int. Ed.*, 2013, **52**, 5377–5381.

11 F. J. Xu and W. T. Yang, *Prog. Polym. Sci.*, 2011, **36**, 1099–1131.

12 H. Yin, R. L. Kanasty, A. A. Eltoukhy, A. J. Vegas, J. R. Dorkin and D. G. Anderson, *Nat. Rev. Genet.*, 2014, **15**, 541–555.

13 B. R. Olden, E. Cheng, Y. L. Cheng and S. H. Pun, *Biomater. Sci.*, 2019, **7**, 789–797.

14 H. P. Fang, Z. P. Guo, L. Lin, J. Chen, P. J. Sun, J. Y. Wu, C. N. Xu, H. Y. Tian and X. S. Chen, *J. Am. Chem. Soc.*, 2018, **140**, 11992–12000.

15 X. Liu, J. J. Xiang, D. C. Zhu, L. M. Jiang, Z. X. Zhou, J. B. Tang, X. R. Liu, Y. Z. Huang and Y. Q. Shen, *Adv. Mater.*, 2016, **28**, 1743–1752.

16 L. H. Wang, D. C. Wu, H. X. Xu and Y. Z. You, *Angew. Chem., Int. Ed.*, 2016, **55**, 755–759.

17 L. Zou, S. Y. Lee, Q. Wu, H. Zhang, A. Bastian, C. Orji, G. Payne, A. Galvez, T. Thomas, Z. Zhang and H. Dou, *J. Biomed. Nanotechnol.*, 2018, **14**, 1785–1795.

18 H. He, N. Zheng, Z. Y. Song, K. H. Kim, C. Yao, R. J. Zhang, C. L. Zhang, Y. H. Huang, F. M. Uckun, J. J. Cheng, Y. F. Zhang and L. C. Yin, *ACS Nano*, 2016, **10**, 1859–1870.

19 D. P. Feldmann, Y. L. Cheng, R. Kandil, Y. R. Xie, M. Mohammadi, H. Harz, A. Sharma, D. J. Peeler, A. Moszczynska, H. Leonhardt, S. H. Pun and O. M. Merkel, *J. Controlled Release*, 2018, **276**, 50–58.

20 M. E. Davis, J. E. Zuckerman, C. H. J. Choi, D. Seligson, A. Tolcher, C. A. Alabi, Y. Yen, J. D. Heidel and A. Ribas, *Nature*, 2010, **464**, U1067–U1140.

21 W. W. Shen, Q. W. Wang, Y. Shen, X. Gao, L. Li, Y. Yan, H. Wang and Y. Y. Cheng, *ACS Cent. Sci.*, 2018, **4**, 1326–1333.

22 J. E. Dahlman, C. Barnes, O. F. Khan, A. Thiriot, S. Jhunjunwala, T. E. Shaw, Y. P. Xing, H. B. Sager, G. Sahay, L. Speciner, A. Bader, R. L. Bogorad, H. Yin, T. Racie, Y. Z. Dong, S. Jiang, D. Seedorf, A. Dave, K. S. Sandhu, M. J. Webber, T. Novobrantseva, V. M. Ruda, A. K. R. Lytton-Jean, C. G. Levins, B. Kalish, D. K. Mudge, M. Perez, L. Abegauz, P. Dutta, L. Smith, K. Charisse, M. W. Kieran, K. Fitzgerald, M. Nahrendorf, D. Danino, R. M. Tuder, U. H. von Andrian, A. Akinc, D. Panigrahy, A. Schroeder, V. Koteliansky, R. Langer and D. G. Anderson, *Nat. Nanotechnol.*, 2014, **9**, 648–655.

23 E. Wagner, *Acc. Chem. Res.*, 2012, **45**, 1005–1013.

24 L. Du, C. Wang, L. Meng, Q. Cheng, J. Zhou, X. Wang, D. Zhao, J. Zhang, L. Deng, Z. Liang, A. Dong and H. Cao, *Biomaterials*, 2018, **176**, 84–93.

25 C. Xu, Y. Z. Z. Zhang, K. Xu, J. J. Nie, B. R. Yu, S. J. Li, G. Cheng, Y. L. Li, J. Du and F. J. Xu, *Nat. Commun.*, 2019, **10**, 3184.

26 H. Lopez-Bertoni, K. L. Kozielski, Y. Rui, B. Lal, H. Vaughan, D. R. Wilson, N. Mihelson, C. G. Eberhart, J. Laterra and J. J. Green, *Nano Lett.*, 2018, **18**, 4086–4094.

27 Y. H. Jiang, Q. Lu, Y. H. Wang, E. Xu, A. Ho, P. Singh, Y. F. Wang, Z. Z. Jiang, F. Yang, G. T. Tietjen, P. Cresswell and W. M. Saltzman, *Nano Lett.*, 2020, **20**, 1117–1123.

28 A. Yen, Y. L. Cheng, M. Sylvestre, H. H. Gustafson, S. Puri and S. H. Pun, *Mol. Pharmaceutics*, 2018, **15**, 2268–2276.

29 S. W. L. Lee, C. Paoletti, M. Campisi, T. Osaki, G. Adriani, R. D. Kamm, C. Mattu and V. Chiono, *J. Controlled Release*, 2019, **313**, 80–95.

30 M. A. Islam, E. K. G. Reesor, Y. J. Xu, H. R. Zope, B. R. Zetter and J. J. Shi, *Biomater. Sci.*, 2015, **3**, 1519–1533.

31 Y. Weng, H. Xiao, J. Zhang, X.-J. Liang and Y. Huang, *Biotechnol. Adv.*, 2019, **37**, 801–825.

32 Y. Zhang, A. Satterlee and L. Huang, *Mol. Ther.*, 2012, **20**, 1298–1304.

33 J. Chen, K. Wang, J. Y. Wu, H. Y. Tian and X. S. Chen, *Bioconjugate Chem.*, 2019, **30**, 338–349.

34 H. C. Kang, K. M. Huh and Y. H. Bae, *J. Controlled Release*, 2012, **164**, 256–264.

35 I. Lostale-Seijo and J. Montenegro, *Nat. Rev. Chem.*, 2018, **2**, 258–277.

36 D. H. Pei and M. Buyanova, *Bioconjugate Chem.*, 2019, **30**, 273–283.

37 E. L. Eskelinen and P. Saftig, *Biochim. Biophys. Acta, Mol. Cell Res.*, 2009, **1793**, 664–673.

38 H. Haisma, *Hum. Gene Ther.*, 2011, **22**, A14–A14.

39 W. Stoorvogel, G. J. Strous, H. J. Geuze, V. Oorschot and A. L. Schwartz, *Cell*, 1991, **65**, 417–427.

40 A. J. Convertine, D. S. W. Benoit, C. L. Duvall, A. S. Hoffman and P. S. Stayton, *J. Controlled Release*, 2009, **133**, 221–229.

41 M. K. G. Jayakumar, A. Bansal, K. Huang, R. Yao, B. N. Li and Y. Zhang, *ACS Nano*, 2014, **8**, 4848–4858.

42 Y. L. Cheng, R. C. Yumul and S. H. Pun, *Angew. Chem., Int. Ed.*, 2016, **55**, 12013–12017.

43 M. Meyer, A. Philipp, R. Oskuee, C. Schmidt and E. Wagner, *J. Am. Chem. Soc.*, 2008, **130**, 3272–3273.

44 M. M. Wang, H. M. Liu, L. Li and Y. Y. Cheng, *Nat. Commun.*, 2014, **5**, 3053.

45 Y. Y. Yuan, C. J. Zhang and B. Liu, *Angew. Chem., Int. Ed.*, 2015, **54**, 11419–11423.

46 J.-P. Behr, *Chimia*, 1997, **51**, 34–36.

47 A. E. Nel, L. Madler, D. Velegol, T. Xia, E. M. V. Hoek, P. Somasundaran, F. Klaessig, V. Castranova and M. Thompson, *Nat. Mater.*, 2009, **8**, 543–557.

48 J. G. Schellinger, J. A. Pahang, R. N. Johnson, D. S. H. Chu, D. L. Sellers, D. O. Maris, A. J. Convertine, P. S. Stayton, P. J. Horner and S. H. Pun, *Biomaterials*, 2013, **34**, 2318–2326.

49 E. J. Kwon, S. Liong and S. H. Pun, *Mol. Pharmaceutics*, 2010, **7**, 1260–1265.

50 J. G. Schellinger, J. A. Pahang, J. L. Shi and S. H. Pun, *ACS Macro Lett.*, 2013, **2**, 725–730.

51 D. J. Peeler, S. N. Thai, Y. L. Cheng, P. J. Horner, D. L. Sellers and S. H. Pun, *Biomaterials*, 2019, **192**, 235–244.

52 B. L. Chen, K. Yoo, W. Xu, R. Pan, X. X. Han and P. Chen, *Drug Delivery Transl. Res.*, 2017, **7**, 507–515.

53 J. J. Chen, J. X. Ding, Y. C. Wang, J. J. Cheng, S. X. Ji, X. L. Zhuang and X. S. Chen, *Adv. Mater.*, 2017, **29**, 1701170.

54 J. Z. Du, T. M. Sun, W. J. Song, J. Wu and J. Wang, *Angew. Chem., Int. Ed.*, 2010, **49**, 3621–3626.